Raman Response of Network Modifier Cations in Alumino-Silicate Glasses

ARTICLE *in* THE JOURNAL OF PHYSICAL CHEMISTRY B · FEBRUARY 2015

Impact Factor: 3.3 · DOI: 10.1021/jp5116299 · Source: PubMed

2 AUTHORS:

Bernard Hehlen
Université de Montpellier
6 PUBLICATIONS **11** CITATIONS
SEE PROFILE

Daniel Neuville
French National Centre for Scientific Research
216 PUBLICATIONS **2,893** CITATIONS
SEE PROFILE

THE JOURNAL OF PHYSICAL CHEMISTRY B

Article

pubs.acs.org/JPCB

Raman Response of Network Modifier Cations in Alumino-Silicate Glasses

B. Hehlen*,† and D. R. Neuville‡

†Laboratoire Charles Coulomb (L2C), UMR 5221 CNRS-Université Montpellier, Montpellier, France

‡CNRS-IPGP, Géomatériaux, 1 rue Jussieu, 75005 Paris, France

ABSTRACT: Raman scattering is performed in three sets of aluminosilicate glasses with light cations and concentrations varying from peralcaline to peraluminate domain. The depolarized spectra highlight two cation modes below ~400 cm^{-1}. Comparison with infrared data reveals very stringent selection rules providing as much additional information for a vibrational analysis. The latter suggests in-phase (network-coupled) and out-of-phase (network-decoupled) displacements of the cations relative to their adjacent negatively charged structures. The low frequency vibration involves all cations whatever their role in the glass, network modifiers or charge compensators. Very interestingly, the second mode originates mostly from cations at modifier's places, providing thereby a new support for structural and chemical analysis of silicate glasses using Raman scattering.

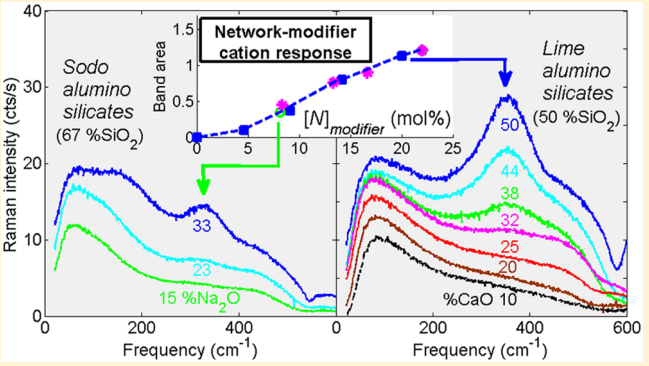

I. INTRODUCTION

The atomic structure of vitreous silica, v-SiO_2, can be regarded eiher by well-defined SiO_4 tetrahedra connected each others by loose bonds at oxygen sites, or by a ramdom distribution of loose Si−O−Si bonds.[1−3] It is the large angular spread of the Si−O−Si angles wich makes the structural disorder in the glass. Inserting alkali ions (e.g., Na) in vitreous silica depolymerizes the SiO_2 network and creates $Si-O^-$ bonds with one cation close to the O^- atom called non bridging oxygen (NBO). Alkali-earth cations (e.g., Ca) carry two positive charges and each cation is therefore located nearby two NBOs. In alkali doped alumino-silicates, alumina acts as glass former over a large concentration range, and AlO_4^- tetrahedra replace SiO_4 tetrahedra in the network. Therefore, the cations can be either network modifiers, as described above, or charge compensators. In the latter situation, they compensate the negative charge carried by the AlO_4^- tetrahedra. RMN has shown that increasing alkali over alumine concentration ratio also induces AlO_5^{2-} (Al^V) and AlO_6^{3-} (Al^{VI}) structures. For the alkali rich region, the proportion of Al^V can go up to 10 mol % of the total concentration of Al_2O_3.[4,5] The structural modifications induced by alkalii and alumina in vitreous silica can also be followed using Raman scattering.[5−7] This spectroscopy has the advantage of being very easy to operate and also very sensitive to weak structural changes and to the medium range order. However, the broad vibrational responses characteristic of disordered materials are often very difficult to analyze and the unknown coupling-to-light coefficients sometimes prevent from quantitative structural descriptions. Beside, Raman scattering in silicate glasses successfully accounts for the modifications of the Q_n structures (SiO_4 units with $4 - n$ NBOs),[8−10] the concentration of 3-fold and 4-fold Si−O−Si rings,[11] and more recently to the Si−O−Si angle in the network and in the small rings.[12]

This article focuses on Raman vibrational responses arising from cation motions. Since cations can be either alkali or alkali-earth, both having two different structural surroundings i.e., modifier-type or charge compensator-type, three family of silicates glasses have been investigated: six sodosilicates (NS) of formula $xSiO_2$−zNa_2O with $z = 100 - x$, three sodoalumino-silicates (NAS) with $x = 67$ mol % SiO_2 and formula $67SiO_2$−zNa_2O−yAl_2O_3, and seven lime aluminosilicates (CAS) with $x = 50$ mol % SiO_2 and formula $50SiO_2$−$zCaO$−yAl_2O_3. In the two ternary glasses the molar concentration of CaO or Na_2O is $z = 100 - (x + y)$. The compositions in a ternary diagram are shown in Figure 1. The ternary glasses stand on an horizontal line emphasizing their constant silica content. They go from the peralcaline, $R = z/y > 1$, to the peraluminate, $R < 1$, zone. The NS glasses are along the alkali to silica join and their composition ranges from 0 to 40 mol % of sodium oxide. In the following they will be noted NSX, with $X = x/z$.

The samples were obtained by melting mixtures of Na_2CO_3, $CaCO_3$, Al_2O_3, and SiO_2. About 100 g of $CaCO_3$−Na_2CO_3−Al_2O_3−SiO_2 (Rectapur from Merck) was ground for 1 h under alcohol in an agate mortar, heated slowly to decompose the carbonates, and then heated above the melting point. These glasses were melted in covered Pt crucibles to avoid contamination. The melts were maintained for a few hours at

Received: November 20, 2014
Revised: February 24, 2015

DOI: 10.1021/jp5116299
J. Phys. Chem. B XXXX, XXX, XXX−XXX

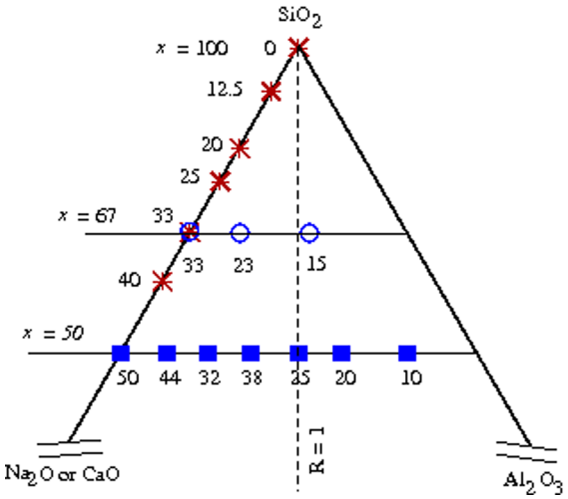

Figure 1. Location of the glass samples in the ternary phase diagram {SiO_2, Na_2O or CaO, Al_2O_3}: sodo silicates (stars), sodoaluminosilicates (squares), and lime alumino silicates (circles). x is the SiO_2 molar concentration, and the numbers close to the symbols indicate the alkali oxide molar content, z. The tectosilicate join ($R = 1$) link the paralcaline domain on the left ($R > 1$) and the peraluminous domain on the right ($R < 1$).

high temperature (1800 K for lime-silicate melt and 1300 K for soda rich silicate melt) in air and stirred to obtain the bubble-free products. The sample was quenched in a few seconds from high temperature by dipping the bottom of the platinum crucible into pure water. The heating procedure was repeated until no crystallization could be detected by optical microscope and X-ray diffractometry. All materials were found to be chemically homogeneous glassy phases before and after viscosity measurements. Glass samples were analyzed using an electron microprobe analyses, Cameca SX100

II. RAMAN SPECTRA

The polarized (VV) and depolarized (VH) Raman spectra were recorded on a T64000 Jobin-Yvon spectrometer working in its triple monochromator mode and with gratings with 1800 grooves/mm. The light from an argon laser emitting at $\lambda = 514$ nm was focused on the sample with a × 100 microscope objective and the scattering was collected in the backscattering geometry. Many care was taken to get intensities in relative units. The spectra have all been recorded under the same optical conditions and with the same incident power. The sample surfaces were of optical quality, and the incoming light was focused inside the samples in such a way to always optimize the Raman signal. Apart from a constant background subtraction by a straight line when required, all the spectra are raw data and did not suffer any intensity corrections.

The polarized (VV) and unpolarized (VH) Raman spectra of our serie of sodosilicate glasses are shown in Figures 2 and 3. One observes the well-known Q_n-structures at high frequency, typically between 900 and 1250 cm^{-1}. Theses modes can be regarded as stretching motions in SiO_4 tetrahedra with 4-n nonbridging oxygens. The higher frequency band around 1100 cm^{-1} mixes Q_3 and Q_4 responses ($Q_{3,4}$), the peak around 950 cm^{-1} corresponds to Q_1 and Q_2 stretchings, and the weak band observed only in NS1.5 (magnified by 7 in Figure 2) to stretchings in fully depolymerized tetrahedra, Q_0. The response from the Q_n species in VH qualitatively reproduces that of the VV spectra, with however differences in the intensity ratios

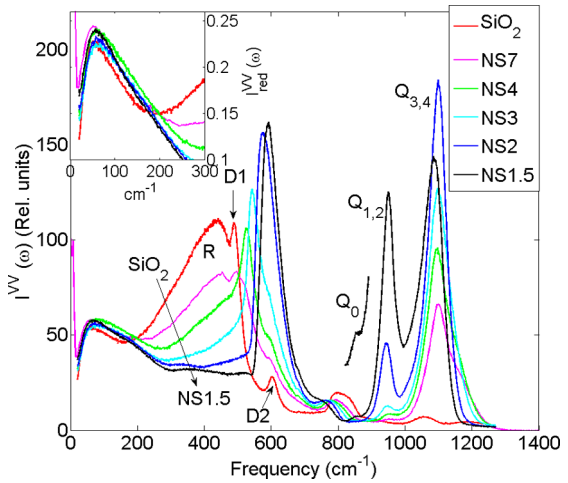

Figure 2. Polarized (VV) Raman spectra of sodo-silicate glasses. The inset zooms on the boson peak region plotted in relative units.

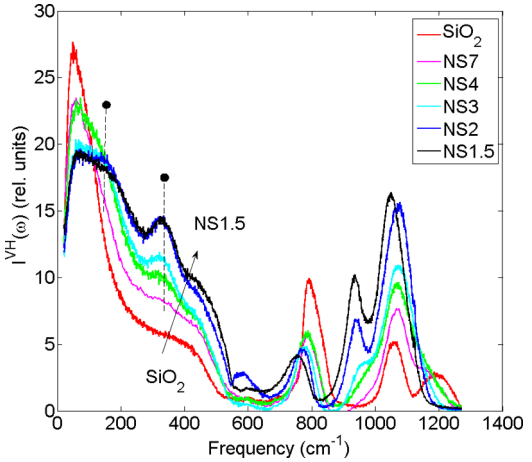

Figure 3. Depolarized (VH) Raman spectra of sodo-silicate glasses. The filled circles point on the two cation modes.

from glass to glass as well as in the frequencies at peak maxima. This emphasizes the complexity of the structure of the modes building each of the three features observed.

The inset of Figure 2 zooms on the boson peak region plotted in reduced intensities, I_{red}^{VV}. $I_{red}(\omega)$ relates to the Raman intensity $I^{RS}(\omega)$ by the relation

$$I_{red}(\omega) \propto \frac{I^{RS}(\omega)}{\omega[n(\omega)+1]} = C(\omega)\frac{g(\omega)}{\omega^2} \quad (1)$$

where $n(\omega)$ is the Bose factor, $g(\omega)$ is the vibrational density of states, and $C(\omega)$ is the coupling-to-light coefficient.[13] For a given mode σ, the latter is given by a suitable projection of the Fourier transform of the correlation function of the dynamical polarizability tensor $\alpha' = \partial\alpha/\partial Q_\sigma$

$$\int \left\langle \frac{\partial\alpha}{\partial Q_\sigma}(\mathbf{r}+\mathbf{r}')\frac{\partial\alpha}{\partial Q_\sigma}(\mathbf{r}') \right\rangle e^{-i\mathbf{q}\mathbf{r}'} d^3\mathbf{r}' \quad (2)$$

$\partial\alpha/\partial Q_\sigma$ is the derivative of the polarizability α over the normal coordinate Q. It is a quantity whose symmetries are known for all point groups and all Raman active modes σ.[14] For modes that are fairly local, such as molecular vibrations, the integral over the position vector $\mathbf{r}$ is independent of the wave vector $\mathbf{q}$.

DOI: 10.1021/jp5116299
J. Phys. Chem. B XXXX, XXX, XXX−XXX

For molecules, the Raman coupling factor C_σ is independent of ω and corresponds to the average of $(\partial\alpha/\partial Q_\sigma)^2$ over all orientations, as discussed in.[14,15] For glasses, the molecular selection rules can be lifted by the structural disorder and in addition C_σ can be frequency dependent, leading to the generic form of the Raman coupling factor $C(\omega)$ in eq 1.

The reduced Raman intensity in eq 1 has the advantage of being proportional to $g(\omega)/\omega^2$ which at low frequency defines the boson peak (BP) in a neutron[16,17] or X-ray[18] inelastic scattering experiment. Interestingly the frequency and shape of the polarized (VV) Raman spectra of the BP evolves very few with sodium concentration. This behavior looks similar in VH (Figure 3) although it is more difficult to observe owing to an additional component (marked by a circle in Figure 3) appearing in the same frequency region.

Bending motions vibrates mostly at intermediate frequencies, between 250 and 600 cm^{-1}. The D1 and D2 bands correspond to O-bending motions in Si−O−Si rings sharing four and three SiO_4 tetrahedra, respectively.[19] The spectral shapes are narrow because these structures are rather well-defined and the vibrations are decoupled from the network. The R-band corresponds to bending motions of Si−O−Si bonds in larger rings. The strong inhomogeneous broadening arises from both the large angular spread of the Si−O−Si structures and the coupling of the vibrations with their neigbhouging units. The intensity of the R-band in VV strongly reduces in the sodo-silicate glasses, and it appears instead a narrow and intense band whose frequency varies from ∼540 cm^{-1} in NS4 to ∼600 cm^{-1} in NS1.5. This behavior emphasizes a reduction of the Si−O−Si angle associated with a sharper spread of its distribution.[15,20] R, D1, and D2 bands are highly polarized and are therefore inactive or very weak in the VH spectra. In the latter, one observes instead a component around 350 cm^{-1} and a second one around 175 cm^{-1} embedded under the boson peak (Figure 3). We will demonstrate in the following that these two features correspond to two different motions of sodium atoms.

To proceed in their analysis, we complemented our NS glass series by two series of alumino silicates glasses, both having a constant silica content (Figure 1): three alkali doped (Na) alumina silicates with x = 67 mol % of SiO_2, $67SiO_2-zNa_2O-yAl_2O_3$ (NAS) and seven alkali-earth doped (Ca) alumino silicates with x = 50 mol % of SiO_2, $50SiO_2-zCaO-yAl_2O_3$ (CAS). The VH spectra up to 600 cm^{-1} are shown in Figure 4. They are dominated by the boson peak at low frequency, at least in the NAS glasses, in which it hinders the observation of the low frequency modes, near 175 cm^{-1}. As qualitatively suggested by a direct observation of Figure 3 and 4, the intensity of the Raman bands at 175 and 350 cm^{-1} clearly increase with cation concentration.

III. MODIFIER AND COMPENSATOR STATE OF CATIONS

Extracting the intensity of the low frequency cation mode from the raw data is very difficult owing to the proximity of the boson peak. Fortunately the latter evolves very few upon cation content, similarly to the NS series. Therefore, in order to reduce its contribution we produced difference spectra by subtracting the raw data by the spectrum having the smallest cation concentration, that is 15 mol % Na_2O ($R = z/y = 0.83$) in the NAS series and 10 mol % CaO (R = 0.25) in the CAS series. The result is shown in Figure 5 for the two remaining NAS glasses and the seven remaining CAS glasses. This

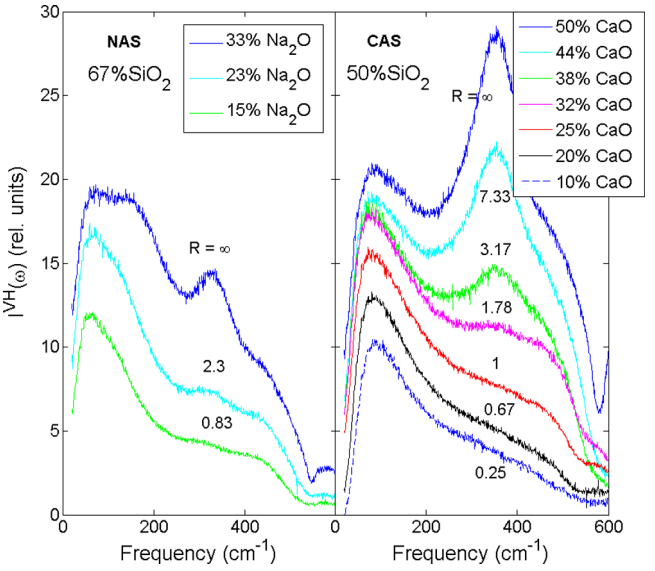

Figure 4. Depolarized (VH) Raman spectra of sodo-alumino-silicate glasses (NAS) with 67 mol % SiO_2 (left) and lime-alumino-silicate glasses (CAS) with 50 mol % SiO_2. The numbers correspond to the cation oxide over alumina oxide concentration ratio, $R = z/y$.

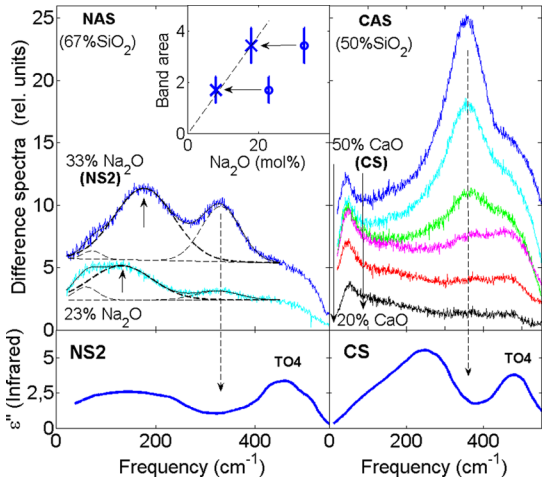

Figure 5. Top panels: Raman difference spectra highlighting the two cations bands in NAS and CAS glasses (see text for details). The low frequency one (150−200 cm^{-1}) appears only in the NAS system. Dashed lines are fits with Gaussian functions. Lower panels: imaginary part of the dielectric constant (ϵ'') obtained from IR data in NS2[21] and in CS.[22] Inset: integrated intensity of the low frequency Raman band of the two NAS difference spectra. The crosses indicate the position of the points after a translation of −15 mol % Na_2O.

treatment first shows that the contribution of the boson peak almost completely vanishes in all the difference spectra, revealing that over the large concentration range explored (keeping the same the silica content), it is wealky affected when substituting alkali oxide by Al_2O_3. This suggests that the Raman activity of the boson peak is dominated by the response of the SiO_4 network. The low Raman efficiency of the alumina network is further evidenced by the fact that no AlO_4 vibrations are observed in our glasses even with as much as 40 mol % Al_2O_3.

A. Cation Band near 175 cm^{-1}. The difference Raman spectra in Figure 5 therefore nicely isolate the two bands under interest. The figure also reproduces the IR spectra of NS2[21] and

DOI: 10.1021/jp5116299
J. Phys. Chem. B XXXX, XXX, XXX−XXX

CS[22] ($50SiO_2$−50CaO) for comparison (bottom panels). One observes the transverse optic mode of lowest frequency (TO4) around 450 cm^{-1}.[23] This is a SiO_2 network vibration inactive (or weakly active) in Raman[15] and it should not be confused to the Raman band around 350 cm^{-1} in the NAS and CAS glasses. The broad IR feature below 300 cm^{-1} appears in many binary silicates and borates glasses and has been assigned to a cation motion since its area is proportional to the cation content.[22,24−26] Its large broadening probably accounts for the different surroundings of the cations, nonbridging oxygens or AlO_4 tetrahedra. The low frequency Raman band in NAS and NS near 175 cm^{-1} (marked by an arrow in Figure 5) is in the same frequency region and exhibits a similar behavior. The inset in Figure 5 shows its area deduced from a Gaussian fit of the difference Raman spectra as a function of sodium concentration. An horizontal translation of −15 mol % shifts the data to the dashed line extrapolating zero for zero Na_2O mol %. Since 15 mol % corresponds to the spectrum used for the subtraction, this result shows that the intensity of the Raman band underneath the boson peak in NAS and NS glasses is proportional to the cation content. This mimics IR observations and therefore confirms that the Raman and IR signatures are likely of same origin.

Interestingly this low frequency polar excitation is not active in Raman in the CAS glasses. This very stringent selection rule is not specific to NAS and CAS glasses but apply to other alkali and alkali-earth aluminosilicates.[27] This constitutes a very important clue for the mode analysis. The polar nature of the mode suggests motions of cations relative to the negative charge carried out by the neighboring oxygen atoms (cation modifier) or AlO_4^- units (cation compensator).[25] The motion of sodium in a X^-Na^+ bond ($X=-O^-$ or AlO_4^-) is Raman active since the fluctuations of the polarizability α over the normal coordinate Q around the equilibrium position, $\alpha' = (\partial\alpha/\partial Q)_0$ is most likely different from zero, and accordingly $C(\omega) \neq 0$ in eq 1. On the contrary, the vibration of calcium relative to its two neighboring X^- structures in a $X^-Ca^{2+}X^-$ bond can be Raman inactive if the bond is linear, since in that case $\alpha(Q)$ is most likely symmetric close to its equilibrium position, and accordingly its derivative is null and $C(\omega) = 0$ in eq 1. It should be noted that the departure from a linear (1D) to a planar (2D) configuration of such YX_2-type bond[28] would activate Raman scattering, a situation which could possibly prevail in glasses with heavy alkali-earth cations. These basic symmetry considerations deserve to be confirmed by numerical simulations. In that perspective, the very specific Raman and IR selection rules pointed-out above provide a very stringent criterion for a cross-checked analysis.

B. Cation Band near 350 cm^{-1}. The Raman band near 350 cm^{-1} also exhibits very stringent selection rules since it is active in Raman *but not* in infrared. It is therefore nonpolar and modulates the dynamical polarizability tensor α'. Contrary to the mode discussed previously, its intensity in the ternary systems decreases much faster than the cation concentration. In the raw data presented in Figure 4 the mode desappears below ~25 mol % CaO in the CAS glasses, that is at the joint $R = z_{CaO}/y = 1$. Within a simplified structural model assuming all aluminum atoms in 4-fold coordinence with every couple of AlO_4^- tetrahedra charge compensated by one calcium atom, the molar concentration of Ca^{2+} cations at network modifier position would be $[N]_{mod} = [N_{Ca}]_{mod} = (z_{CaO} - y)/\text{atm}$, where atm is the number of atoms per mole. The joint $R = z_{CaO}/y = 1$ therefore corresponds to the limit below which exist calcium atoms acting as network modifiers ($R < 1$) and above which all cations are at charge compensator positions ($R > 1$). In the NAS system one single AlO_4^- tetrahedra is charge compensated by one Na^+ cation and the molar concentration of Na^+ cations at network modifier position is $[N]_{mod} = [N_{Na}]_{mod} = 2(z_{Na2}O - y)/\text{atm}$. Accordingly the joint $R = z_{Na_2O}/y = 1$ still corresponds to concentrations above which all sodium atoms are at charge compensator position. The amount of 5-fold and 6-fold coordinated Al atoms should not exceed few percents in our glasses[4] and for sake of simplicity those structures have not been taken into account in the analysis below.

The Raman spectra near 350 cm^{-1} in Figure 3 and 4 have been fitted using a Gaussian function accounting for the cation mode, and an exponential decay locally accounting for the broad underlying signal arising from the tail of the boson peak. The choice of the latter is arbitrary provided the fitting parameters vary smoothly and continuously from glass to glass. The Raman response of the cation band reduced from this underlying BP contribution is shown in Figure 6. The

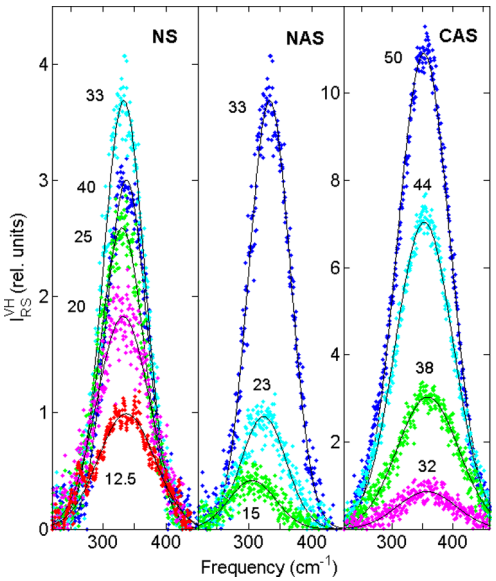

Figure 6. High frequency cation band extracted from the VH spectra and its fit with a Gaussian function. The numbers correspond to the cation concentration.

integrated intensities resulting from the Gaussian fits (also shown in Figure 6) are shown in Figure 7a as a function of the alkali oxide content z. Example of errorbars estimated from the fit are displayed. They are large when $[N]_{mod}$ tends to zero in the sodo-silicates because the Raman responses are weak and their fitting become sensible to the signal arising from the BP. The Raman signal is much larger in the CAS glasses (the intensities have been divided by 4.2 in Figure 7) giving rise to errors about the size of the symbols. The arrows mark the tectosilicate join ($R = 1$) for the three series: $z = 0$, 16.5, and 25 mol % for NS, NAS and CAS glasses, respectively. In the sodo-silicate glasses, the intensity varies quasi linearly with sodium content, except for NS1.5 whose value deviates from the general trend (Figure 7a). The signal naturally extrapolates to zero for $z = 0$ in the binary system as expected for a band originating from cation motions. Very interestingly, the mode completely vanishes in the CAS glasses for CaO concentrations below 25 mol % as pointed above by looking directly on the

DOI: 10.1021/jp5116299
J. Phys. Chem. B XXXX, XXX, XXX−XXX

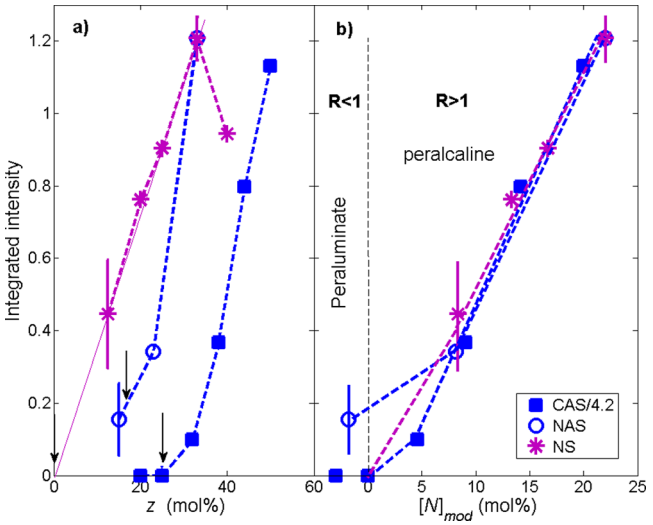

Figure 7. Integrated intensity of the cation band near 350 cm^{-1}, plotted (a) as a function of the total alkali oxide content z (in mol %) and (b) as a function of modifier cations content $[N]_{mod}$ (in mol %). Dashed lines connect glasses of the same family and the arrows point to the concentrations at the tectosilicate join (R = 1). In both panels, the intensities of the CAS glasses have been divided by 4.2.

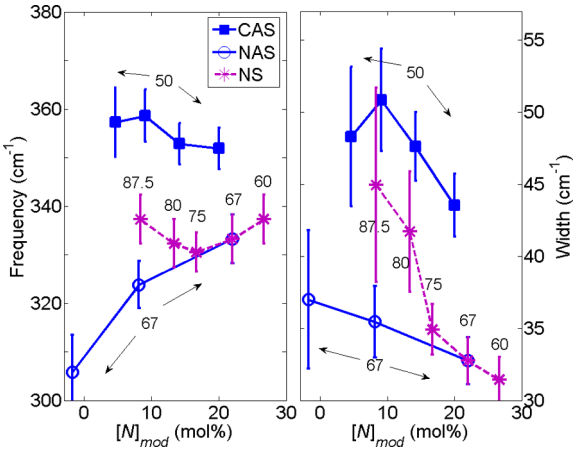

Figure 8. (a) Frequency and (b) width as a function of the molar concentration of modifier cations $[N]_{mod}$. Full and dashed lines connect glasses of the same family. The numbers correspond to the mol % of SiO_2.

raw spectra. This exactly corresponds to the join R = 1 where all cations are charge compensators whithin the simple structural model presented above, demonstrating thereby that the mode arises from Ca motions at modifier's place. The situation in NAS is intermediate, since a weak contribution remains below the tectosilicate join. However, the fact that for similar sodium concentrations, the signal is much weaker in the NAS than in the NS glasses supports the above assumption that the vibration mostly associates to cations at modifier's place, with presumably in that case a very weak contribution from compensator cations in the same frequency region. It therefore makes sense presenting the same integrated intensities as a function of the molar concentration of modifier cations, $[N]_{mod}$ (Figure 7b). The results for the CAS glasses have been divided by 4.2 in order to match with the curves of the sodosilicates at high $[N]_{mod}$. The negative values of $[N]_{mod}$ correspond to a situation where all cations are charge compensators. Contrary to the representation of Figure 7a, the three curves now exhibit a very similar behavior confirming that the mode relates specifically to cations at modifier's place and not to the total number of cations in the glass. Hence, it likely involves $-O^-Na^+$ motions in the sodo-silicates (NS and NAS), and $-O^-Ca^{2+}O^-$– motions in the lime-silicates (CS, CAS). The nonpolar nature of the vibration (IR inactive, see Figure 5) suggests that contrary to the low frequency band originating from network-decoupled cation motions, this one could involve the cation together with its surrounding oxygen(s) in an overall motion defining thereby a network-coupled vibration.

Finally, the frequency and width of the mode is presented in Figure 8. Since the vibration associates to modifier cations, the data are presented as a function of $[N]_{mod}$ rather than the total cation content. The figures close to the points refer to silica concentrations. The frequency of the NS glasses exhibits a minimum for NS3 (z_{Na_2O} = 25), eventually accompanied by an increase of the line width at low $[N]_{mod}$. Interestingly, this concentration is close to the value at which a transition from a rigid (stressed) phase (z < 18) toward a floppy phase (z > 23) was observed.[29] The overall trend is similar in NS and CAS but different in the NAS glasses, in particular concerning the frequency which behave in an opposite way. The strong frequency decrease in the latter supports or previous statement of a change in the nature of the mode when passing from peraluminate ($[N]_{mod}$ > 0) to peralcaline compositions. The very weak remaining signal when no more Na atoms are supposed to by at modifier's place could therefore originates from a vibration of cations at compensators position. The motion could for instance involve $AlO_4^-Na^+$ structures in an overall motion. Such a vibration is not likely in calcium doped aluminosilicates since one cation is attached to two AlO_4^- tetrahedra giving rise to a much harder motion, if any.

IV. CONCLUSION

Polarized and depolarized Raman scattering have been performed in three sets of aluminosilicate glasses and the results have been compared to infrared absorption data. Two modes associated with cation motions are observed at low frequency in the vibrational responses. Depending on the glass composition, they are active in Raman or in infrared absorption, or both. Aside from the main purpose of that study, the Raman spectroscopy revealed that for each glass family, the shape and frequency of the boson peak evolves very few within the large cation and alumina concentration range explored. This suggests a Raman activity of the BP dominated by the response of the silica network.

Our analysis concentrates on the depolarized Raman spectra where the strong R-band is absent providing thereby a much better situation for the observation of the two cation modes. The spectroscopy emphasizes pronounced selection rules and cation-site dependent Raman intensities. The lowest frequency vibration at 150–250 cm^{-1} involves both modifier and charge compensator cations while the second around 340–360 cm^{-1} mostly originates from cations at modifier's place. The former is associated with a motion of the cation relative to its adjacent negative charge(s) (carried either by the NBOs or the AlO_4^- tetrahedra). If the cation is attached to one negative charge (alkali case) the vibration is Raman active since it modulates the polarizability. On the contrary, if the cation is surrounded by two negative charges (alkaline earth elements), the motion is symmetric (perfectly symmetric in case of a linear YX_2 unit) and the mode becomes silent in Raman. In both case the

DOI: 10.1021/jp5116299
J. Phys. Chem. B XXXX, XXX, XXX–XXX

vibrations modulate the dipole moment and are IR active. The mode arising from network modifier cations (340−360 cm^{-1}) appears in Raman in all glasses investigated. It is nonpolar (IR-inactive) and is assigned to a motion involving $-O^{-}Na^{+}$ and $-O^{-}Ca^{2+}O^{-}-$ structures in an averall motion. The analysis therefore suggests that the vibrations of cations at low frequency can be regarded as a combination of out-of-phase motions (low-frequency mode) and in-phase motions (high frequency mode) of the cations relative to the adjacent negative charge(s) connecting them to the network. The present study has been performed in glasses with light cations and it is not clear how these conclusions transpose in case of heavy cations.

AUTHOR INFORMATION

Corresponding Author

*(B.H.) E-mail: bernard.hehlen@univ-montp2.fr.

Notes

The authors declare no competing financial interest.

REFERENCES

(1) Mozzi, R. L.; Warren, B. E. The structure of vitreous silica. *J. Appl. Crystallogr.* **1969**, *2*, 164−172.

(2) Wright, A. C. Neutron scattering from vitreous silica. The structure of vitreous silica: What have we learned from 60 years of diffraction studies? *J. Non-Cryst. Solids.* **1994**, *179*, 84−115.

(3) Taraskin, S. N.; Elliott, S. R. Nature of vibrational excitations in vitreous silica. *Phys. Rev. B* **1997**, *56*, 8605−8622.

(4) Neuville, D. R.; Cormier, L.; Montouillout, V.; Massiot, D. Local environment of Al in aluminosilicate glasses: a NMR point of view. *J. Non-Cryst. Solids* **2007**, *353*, 180−185.

(5) Neuville, D. R.; Cormier, L.; Montouillout, V.; Florian, P.; Millot, F.; Rifflet, J. C.; Massiot, D. Structure of Mg and Mg/Ca aluminosilicate glasses: ^{27}Al NMR and Raman spectroscopy investigations. *Am. Mineral.* **2008**, *93*, 1721−1731.

(6) Sharma, S. K.; Philpotts, J. A.; Matson, D. W. Ring distributions in alkali- and alkaline-earth aluminosilicate framework glasses - a raman spectroscopic study. *J. Non-Cryst. Solids* **1985**, *71*, 403−410.

(7) Daniel, I.; Gillet, P.; Poe, B. T.; McMillan, P. F. In-situ High-Temperature Raman Spectroscopic Studies of Aluminosilicate Liquids. *Phys. Chem. Minerals* **1995**, *22*, 74−86.

(8) McMillan, P. F. Structural studies of silicate glasses and melts-applications and limitations of Raman spectroscopy. *Am. Mineral.* **1984**, *69*, 622−644.

(9) Mysen, B. O.; Frantz, J. D. Structure and properties of alkali silicate melts at magmatic temperatures. *Eur. J. Mineral.* **1993**, *5*, 393−407.

(10) Mysen, B. O. Experimental, in situ, high-temperature studies of properties and structure of silicate melts relevant to magmatic processes. *Eur. J. Mineral.* **1995**, *7*, 745−766.

(11) Burgin, J.; Guillon, C.; Langot, P.; Vallée, F.; Hehlen, B.; Foret, M. Vibrational modes and local order in permanently densified silica glasses: Femtosecond and Raman spectroscopy study. *Phys. Rev. B* **2008**, *78*, 184203−184203−9.

(12) Hehlen, B. Inter-tetrahedra bond angle of permanently densified silicas extracted from their Raman spectra. *J. Phys.: Condens. Matter* **2010**, *22*, 025401−025401−6.

(13) Shuker, R.; Gammon, R. W. Raman-scattering selection-rule breaking and the density of states in amorphous materials. *Phys. Rev. Lett.* **1970**, *25*, 222−225.

(14) Cyvin, S. J.; Rauch, J. E.; Decius, J. C. Theory of Hyper-Raman Effects (Nonlinear Inelastic Light Scattering): Selection Rules and Depolarization Ratios for the Second-Order Polarizability. *J. Chem. Phys.* **1965**, *43*, 4083−4095.

(15) Hehlen, B.; Simon, G. The vibrations of vitreous silica observed in hyper-Raman scattering. *J. Raman. Spectrosc.* **2012**, *43*, 1941−1950.

(16) Buchenau, U.; Nuecker, N.; Dianoux, A. J. Neutron scattering study of the vibration-relaxation crossover in amorphous polycarbonates. *Phys. Rev. Lett.* **1984**, *53*, 2316−2319.

(17) Buchenau, U.; Prager, M.; Nuecker, N.; Dianoux, A. J.; Ahmad, N.; Philips, W. A. Low-frequency modes in vitreous silica. *Phys. Rev. B* **1986**, *34*, 5665−5673.

(18) Rufflé, B.; Guimbretière, G.; Courtens, E.; Vacher, R.; Monaco, G. Glass-Specific Behavior in the Damping of Acousticlike Vibrations. *Phys. Rev. Lett.* **2006**, *96*, 045502−045502−4.

(19) Umari, P.; Gonze, X.; Pasquarello, A. Concentration of small ring structures in vitreous silica from a first-principles analysis of the Raman spectrum. *Phys. Rev. Lett.* **2003**, *90*, 27401−27405.

(20) Hehlen, B., Neuville, D., Ispas, S., to be published.

(21) Merzbacher, C. I.; White, W. B. Structure of Na in aluminosilicate glasses: A far-infrared reflectances spectroscopics study. *Am. Mineral.* **1988**, *73*, 1089−1094.

(22) De Sousa Meneses, D.; Malki, M.; Echegut, P. Optical and structural properties of calcium silicate glasses. *J. Non-Cryst. Solids* **2006**, *352*, 5301−5308.

(23) Kirk, C. T. Quantitative analysis of the effect of disorder-induced mode coupling on infrared absorption in silica. *Phys. Rev. B* **1988**, *38*, 1255−1273.

(24) Kapoutsis, J. A.; Kamitsos, E. I.; Chryssikos, G. D.; Yiannopoulos, Y. D. Proceedings of the International Symposium on Glass Science and Technology. *Chim. Chron. New Ser.* **1994**, *23*, 341−346.

(25) Kamitsos, E. I.; Patsis, A. P.; Chryssikos, G. D. Infrared reflectance investigation of alkali diborate glasses. *J. Non-Cryst. Solids* **1993**, *152*, 246−257.

(26) De Sousa Meneses, D.; Eckes, M.; Del Campo, L.; Santos, C. N.; Vaills, Y.; Echegut, P. Investigation of medium range order in silicate glasses by infrared spectroscopy. *Vib. Spectrosc.* **2013**, *65*, 50−57.

(27) Le Losq, Ch.; Neuville, D. R.; Florian, P.; Henderson, G. S.; Massiot, D. Role of Al3+ on rheology and nano-structural changes of sodium silicate and aluminosilicate glasses and melts. *Geochim. Cosmochim. Acta* **2014**, *126*, 495−517.

(28) Herzberg, G. *Molecular spectra and molecular structures II: infrared and Raman spectra of polyatomic molecules*; Krieger Publishing Company: Malabar, FL, 1991.

(29) Vaills, Y.; Qu, T.; Micoulaut, M.; Chaimbault, F.; Boolchand, P. Direct evidence of rigidity loss and self-organisation in silicate glasses. *J. Phys.: Condens. Matter* **2005**, *17*, 4889−4896.

DOI: 10.1021/jp5116299
J. Phys. Chem. B XXXX, XXX, XXX−XXX